Toward an Animal Model of the Human Tear Film: Biochemical Comparison of the Mouse, Canine, Rabbit, and Human Meibomian Lipidomes

Igor A. Butovich,[1,2] *Hua Lu,*[1,4] *Anne McMahon,*[1,4] *and J. Corinna Eule*[3]

PURPOSE. Secretions that are produced by meibomian glands (also known as meibum) are a major source of lipids for the ocular surface of humans and animals alike. Many animal species have been evaluated for their meibomian lipidomes. However, there have been a very small number of studies in which the animals were compared with humans side by side. Therefore, the purpose of this study was to compare meibum collected from humans and three typical laboratory animals, canines, mice, and rabbits, for their meibomian lipid composition in order to determine which animal species most resembles humans.

METHODS. High pressure liquid chromatography (HPLC) and gas-liquid chromatography (GLC) in combination with mass spectrometry were used to evaluate lipidomes of all tested species.

RESULTS. Among three tested animal species, mice were found to be the closest match to humans in terms of their meibomian lipidomes, while canines were the second closest species. The lipids of these three species were close to each other structurally and, for most lipid classes, quantitatively. The rabbit meibomian lipidome, on the other hand, was vastly different from lipidomes of all other tested species. Interestingly, a previously described class of lipids, acylated omega-hydroxy fatty acids (OAHFA), was found to be present in every tested species as the major amphiphilic component of meibum.

CONCLUSIONS. Our side by side comparison of the rabbit and the human meibum demonstrated their vast differences. Thus, the rabbit seems to be a poor animal model of the human tear film, at least when studying its biochemistry and biophysics. (*Invest Ophthalmol Vis Sci.* 2012;53:6881–6896) DOI:10.1167/iovs.12-10516

The preocular tear film (TF) is a complex and dynamic structure that protects the human ocular surface from desiccating and from potentially hazardous environmental factors.[1] The TF is composed primarily of three components: lipids, proteins, and aqueous tears. Lipids that are found in the TF are produced largely (but not exclusively[2–4]) by meibomian glands.[5,6] Meibomian lipids (also called meibum[7]) were demonstrated to be a critical component of the TF.[8–10] They are believed to form its outermost part called the TF lipid layer (TFLL).[11] Changes in its biochemistry, for example, in the lipid composition of meibum and TFLL, have been linked to the onset of several pathological ocular conditions, including a multifactorial disease generally termed dry eye (DE).[12] One of the physiological signs of DE is a decreased stability of the TFLL, which can be semi-quantitatively characterized by a decrease in the TF breakup time (TFBUT).[13] These biochemical and physiological changes were evaluated in numerous human studies. However, for understandable reasons, no truly invasive in vivo techniques (such as genetic alterations, surgeries, or aggressive drug treatment) could have been used with live human subjects, which either limited the scope of the in vivo studies, or forced the researchers to resort to post mortem experiments.[7] Thus, there is a clear need to develop and validate a suitable animal model that could be used in experimental studies of the normal TF and TFLL and to model biochemical and biophysical changes that occur upon the onset of DE disease in humans.

Over a period of several decades, meibum from many animal species have been tested and described with varying degrees of particularization. The tested species included the steer, the gerbil, the rat, the rabbit, the dog, the hamster, and the mouse.[7,14–22] The approaches used in those studies included various types of chromatography and, in the later studies, mass spectrometry. In most of the studies where structural information on lipids was to be obtained, the lipids were hydrolyzed to make them suitable for subsequent chromatographic analysis. Note that the method of choice in those earlier studies was gas–liquid chromatography (GLC) with either flame ionization (FI) or mass spectrometric (MS) detection. The only attempt to use high pressure liquid chromatography with MS detection (HPLC/MS) was undertaken by McFadden et al.,[23] who analyzed steer meibum and provided important insight on the molecular structures of wax esters (WE) present in bovine meibum.

In our recent paper[14] we have presented data on the comprehensive comparative lipidomic analysis of canine and human meibum. The experiments were conducted by HPLC/MS using an ion trap mass detector capable of multistage fragmenting parent and daughter ions. The two species were found to be quite similar with regard to their meibomian lipidomes. This information can be helpful in treating dogs, which, like humans, are prone to DE.[24] However, obvious ethical concerns limit the scope of experimental studies that

From the [1]Department of Ophthalmology and [2]The Graduate School of Biomedical Sciences, University of Texas Southwestern Medical Center, Dallas, Texas; and the [3]Klinik und Poliklinik für kleine Haustiere, Freie Universität, Berlin, Germany.

[4]These authors contributed equally to the work presented here and should therefore be regarded as equal authors.

Disclosure: **I.A. Butovich**, None; **H. Lu**, None; **A. McMahon**, None; **J.C. Eule**, None

Corresponding author: Igor A. Butovich, Department of Ophthalmology, University of Texas Southwestern Medical Center, 5323 Harry Hines Boulevard, Dallas, TX 75390-9057; igor.butovich@utsouthwestern.edu.
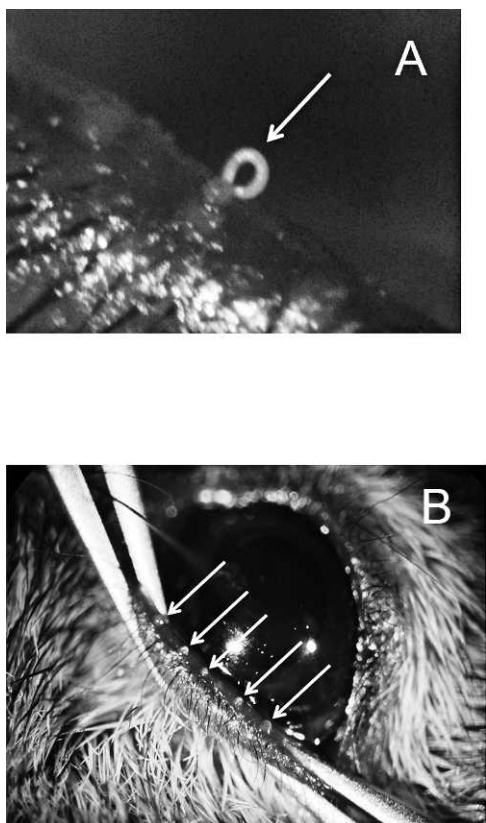
FIGURE 1. Mouse meibum at room (A) and physiological (B) temperatures. *White arrows* show the mouse's meibomian gland orifices with expressed meibum. Notice the changes in appearance of the secretions with temperature (bodily temperature versus ~20°C).

However, even these two species were distinctively different from humans.

Surprisingly, we have been able to find only one publication in relation to lipidomic analysis of mouse meibum. Harvey et al.[15] utilized the GLC/MS technique to characterize the mouse meibomian lipids. Customary to this technique, in the majority of the analyses the lipids were hydrolyzed first and then methylated and/or trimethylsilylated. Thus, only the structures of the resulting free sterols (St), fatty alcohols (FAl), and fatty acids (FA) were evaluated. The authors demonstrated that a large number of FA and FAl were either iso- or anteiso-branched, or unsaturated. The major sterol was found to be cholesterol (Chl). A limited attempt was made to analyze underivatized WE, which showed a high degree of branching and unsaturation of the compounds. No other lipid species were analyzed and/or described in the paper.

With this limited information in hand, it became clear that the mouse meibum (as it was described by Harvey et al.[15]) could be a good candidate for further in depth lipidomic studies, because human meibum also demonstrates a high degree of branching and unsaturation.[7,25] Importantly, the mouse's TFBUT was found to be approximately 6 seconds,[26] which is very close to the human normal TFBUT of at least 10 seconds and above.[27] These numbers provided a clear evidence of physiological similarities between human and mouse TF and TFLL. Therefore, we decided to evaluate in details the meibomian lipidome the mouse (*Mus musculus domestica*) and compare it side by side with meibomian lipids of humans, rabbits (*Oryctolagus cuniculus*), and canines (*Canis lupus familiaris*), using contemporary approaches such as HPLC/API- dual stage mass spectrometry (MS/MS) and GLC/MS/MS to determine which animal species would be best suited for future in-depth TF and TFLL studies.

MATERIALS AND METHODS

Lipid standards were purchased from Nu-Chek Prep, Inc. (Elysian, MN), Matreya, Inc. (Pleasant Gap, PA), and Sigma-Aldrich (St. Louis, MO). HPLC- and spectroscopy-grade solvents were from Honeywell Burdick & Jackson (Morristown, NJ) and Sigma-Aldrich.

GLC/MS experiments were conducted using a Trace GC Ultra gas chromatograph with an ITQ1100 mass spectrometric detector (both from ThermoElectron, San Jose, CA) as described earlier.[25] HPLC/MS experiments were conducted using a Waters 2695 Alliance HPLC system (Waters, Milford, MA) and an LCQ Deca XP Max ion trap mass spectrometer (ThermoElectron).

can be performed on canines, which prompted us to explore other potential candidates among common experimental animals. A few years ago we presented a preliminary report on comparative analysis of meibum samples collected from approximately 10 different species that varied from human to cat to cow to several species of marsupials (Butovich IA, et al. *IOVS* 2009;50:ARVO E-Abstract 2545). None of the tested animal species replicated human meibum. The closest matches in those studies were found to be the cat and the cow.
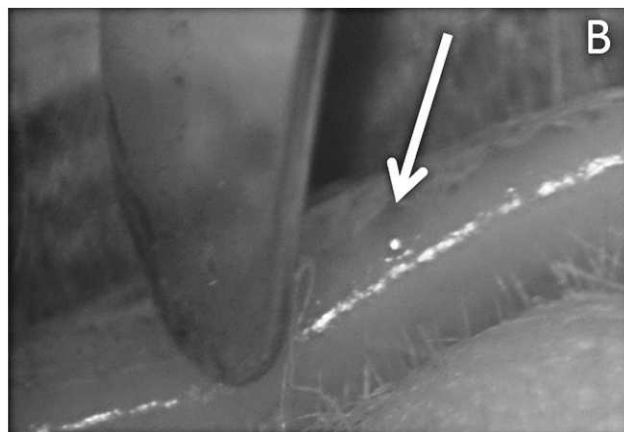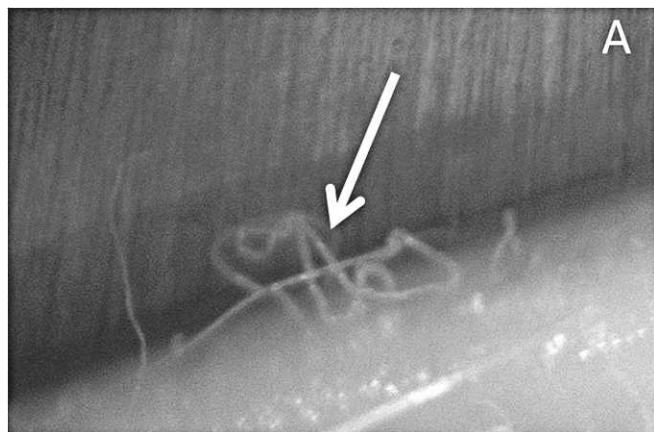

FIGURE 2. Rabbit meibum at room (A) and physiological (B) temperatures. Note that, as with mice, the physical appearance of the secretions changes with temperature.
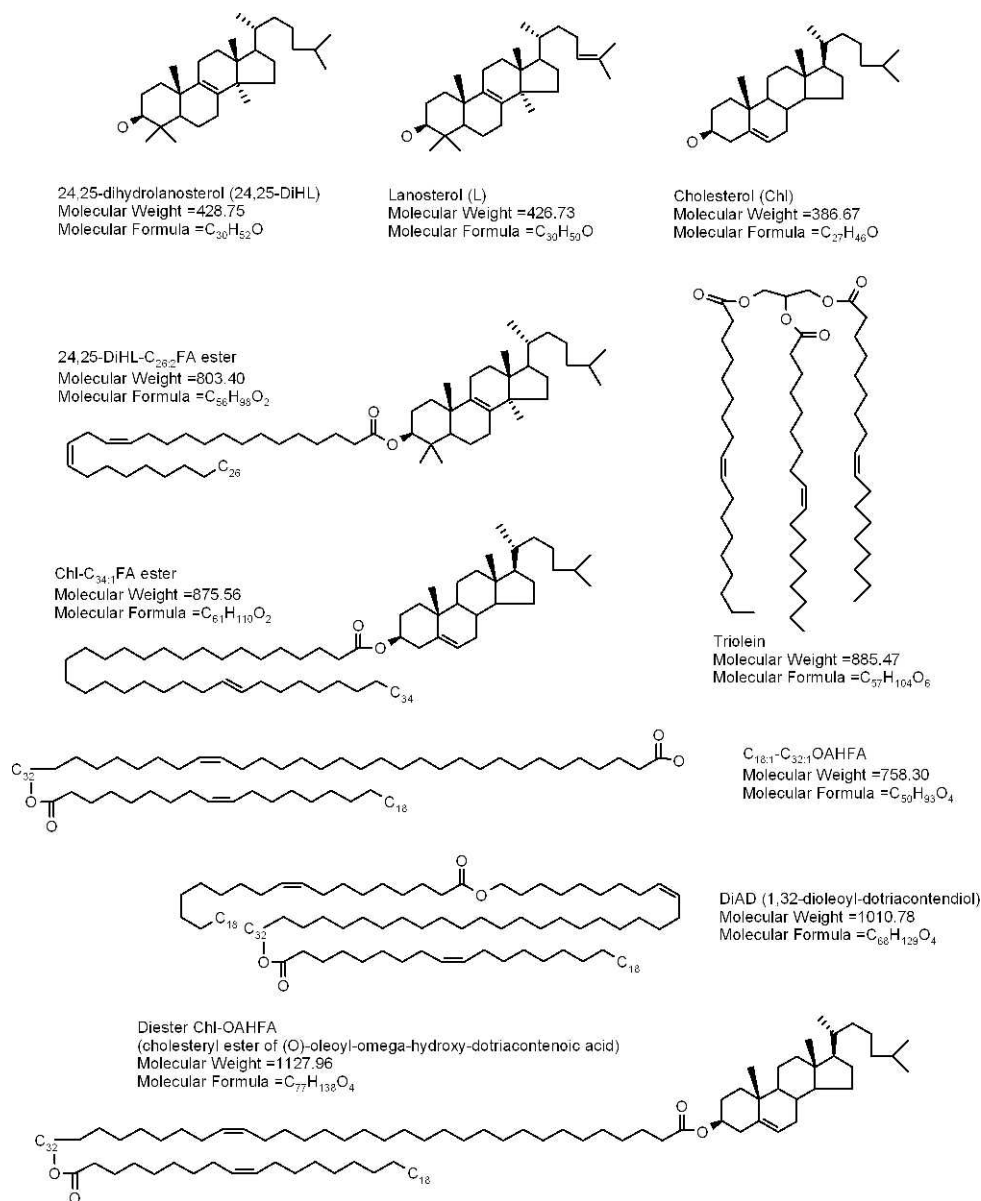
FIGURE 3. Representative lipid species detected in animal and human meibum.

Histology of Meibomian Glands

Mice were euthanized and eyelids fresh frozen in Tissue-Tek Optimum Temperature Cutting Compound (OCT) Tissue was sectioned at 10 μm, mounted and post fixed for 20 minutes with 4% paraformaldehyde in 50 mM PBS (pH 7.4), washed with PBS, and then blocked with 1% bovine serum albumin (BSA) in PBS for 40 minutes. Samples were then incubated overnight at 4°C with sterile biotin-duramycin in PBS (20 mg/mL),[28] followed by washing with PBS, and incubation with DyLight 488 conjugated streptavidin (Thermo Scientific, Rockford, IL) for 1 hour. After removal of unbound streptavidin with PBS the sections were fixed with 2% paraformaldehyde for 10 minutes, washed with PBS, and mounted with Gel/Mount (Biomedia Corp., Foster City, CA). Labeled sections were imaged on an SP2 laser scanning confocal microscope (Leica Microsystems, Heidelberg, Germany) as described previously.[29]

Eyelids for total lipid staining were removed, post fixed in 4% paraformaldehyde at 25°C for 1 hour and overnight at 4°C, followed by successive incubation in 10%, 20%, and 30% sucrose, prior to placing in OCT. Tissue sections (15 μm) were incubated with PBS to remove OCT, rinsed in 50% propan-2-ol for 5 minutes, followed by staining with Oil Red-O (ORO) using a working stock freshly prepared by diluting 6:4 with water from a 0.5% ORO stock in propan-2-ol, which had been heated for 1 hour at 56°C. Following removal of excess, ORO sections were stained with hematoxylin, washed, and mounted with Gel mount.

Collection of Meibomian Lipids

All procedures that involved human subjects had been approved by the University of Texas (UT) Southwestern Medical Center institutional review board and were conducted in accordance with the Declaration of Helsinki. All procedures that involved mice had been approved by the UT Southwestern Institutional Animal Care and Use Committee (certified by the Association for Assessment and Accreditation of Laboratory Animal Care [AAALAC]), and were conducted in accordance with the ARVO Statement for the Use of Animals in Ophthalmic and Vision Research.
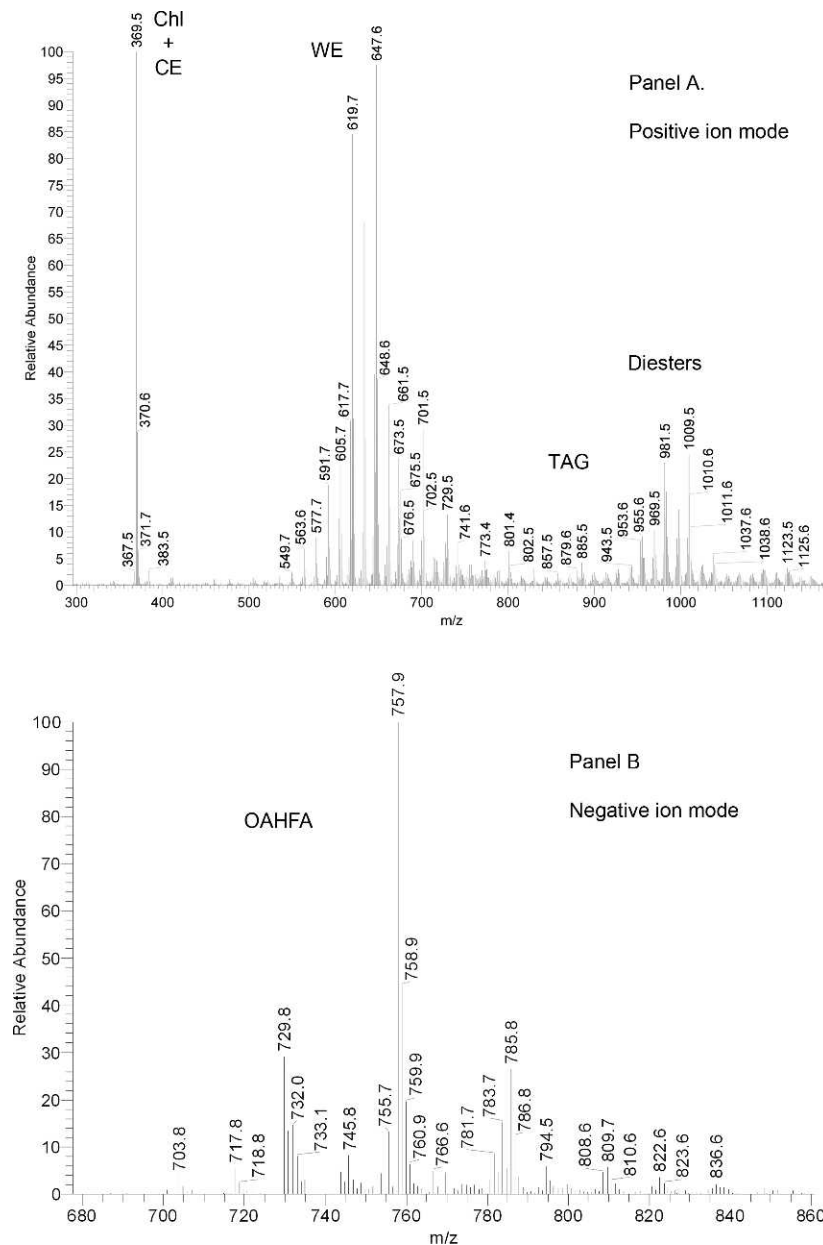
FIGURE 4. Representative mass spectra of human meibum. (**A**) Positive ion mode atmospheric pressure chemical ionization mass spectrum of meibum. (**B**) Negative ion mode atmospheric pressure chemical ionization mass spectrum of meibum.

Human meibum was collected from 12 healthy, non–DE volunteers (average age 37 ± 7 years; seven males and five females[25]) who underwent standard evaluation by a trained ophthalmologist for any ocular surface pathology. To be eligible for the study, the volunteers had to complete a questionnaire and undergo slit lamp evaluation. The following tests (with eligibility criteria) were conducted: TFBUT measurement (only patients with TFBUT of more than 10 seconds were enrolled), Lissamine Green staining (zero on a four-grade scale was acceptable), Schirmer test (>10 mm was required), meibum expressibility (only zero on a five-grade scale was passable), and the meibomian gland evaluation. Meibum was collected by soft squeezing the lower eyelids of the subjects with two cotton swabs, and collecting the expressed meibum with a platinum spatula as described and illustrated earlier.[2,25] The collected sample then was dissolved in approximately 1 mL of a chloroform-methanol solvent mixture (3:1, vol/vol) placed in a preweighed HPLC-style 2-mL glass vial with a

Teflon-lined cap (Waters, Milford, MA). The solvent then was evaporated to dryness, and the vial with the dry sample was reweighed to determine how much dry lipid material had been collected. A typical collected sample weighed approximately 0.6 mg. For the purpose of long term storage, the vial with the sample was flushed with dry, high-purity nitrogen, sealed, and stored at −80°C. Just before the analysis, the sample was dissolved in a proper solvent for either GLC/MS, or HPLC/MS studies.

Adult mice, of both sexes ($n = 10$; five males and five females), on a mixed predominantly 129SvEv and C57Bl/6 background were used for meibum collection and TFBUT measurements. Mice were euthanized immediately before the meibum collection, their eyelashes removed and the upper and lower eyelids sniped on their periphery to create eyelid flaps containing the meibomian glands. Meibum was expressed from the glands by application of gentle pressure along both surfaces of the eyelids, starting below the furthest extremity of the glands. The
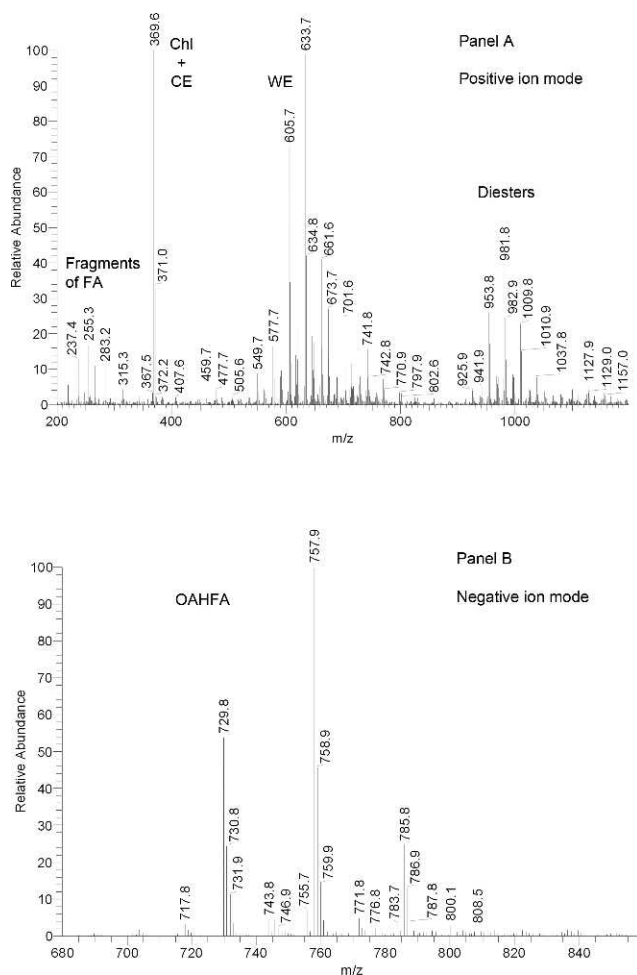
FIGURE 5. Representative mass spectra of canine meibum. (**A**) Positive ion mode atmospheric pressure chemical ionization mass spectrum of meibum. (**B**) Negative ion mode atmospheric pressure chemical ionization mass spectrum of meibum.

FIGURE 6. Representative mass spectra of rabbit meibum. (**A**) Positive ion mode atmospheric pressure chemical ionization mass spectrum of meibum. (**B**) Negative ion mode atmospheric pressure chemical ionization mass spectrum of meibum.

physical appearance of the expressed meibum specimen depended on its temperature: the lower the temperature, the more solid the samples appeared (Fig. 1). Expressed meibum was collected from the eyelid margin and dissolved in a solution of chloroform:methanol equaling 3:1 (vol/vol) and stored as described above for human samples. The amount of collected meibum from an individual animal was sufficient for routine HPLC/MS and GLC/MS evaluation of meibomian lipids. However, for a more detailed lipidomic analysis that involved structural evaluation of minor lipid species, pooled samples from several littermates were used.

Samples of canine meibum (*n* = 10) were those collected for our previous study.[14] Meibum was collected from live animals in a veterinary clinic by a trained veterinarian. The samples were stored under nitrogen at −80°C. No changes in samples were observed since they had been collected and analyzed two years ago.

The rabbit samples (*n* = 7) were collected in-house from female New Zealand white rabbits. The healthy animals had been used in unrelated studies and euthanized afterwards. Within 1 hour after the animals had been euthanized, their eyelids were surgically removed and the meibomian samples were extracted under a surgical microscope using a platinum spatula and two cotton applicators (Fig. 2). Note the effect of the specimen's temperature on the appearance of the samples: when the tissue was at room temperature, meibum had a "hair-like" appearance (Fig. 2A), while at temperatures close to the
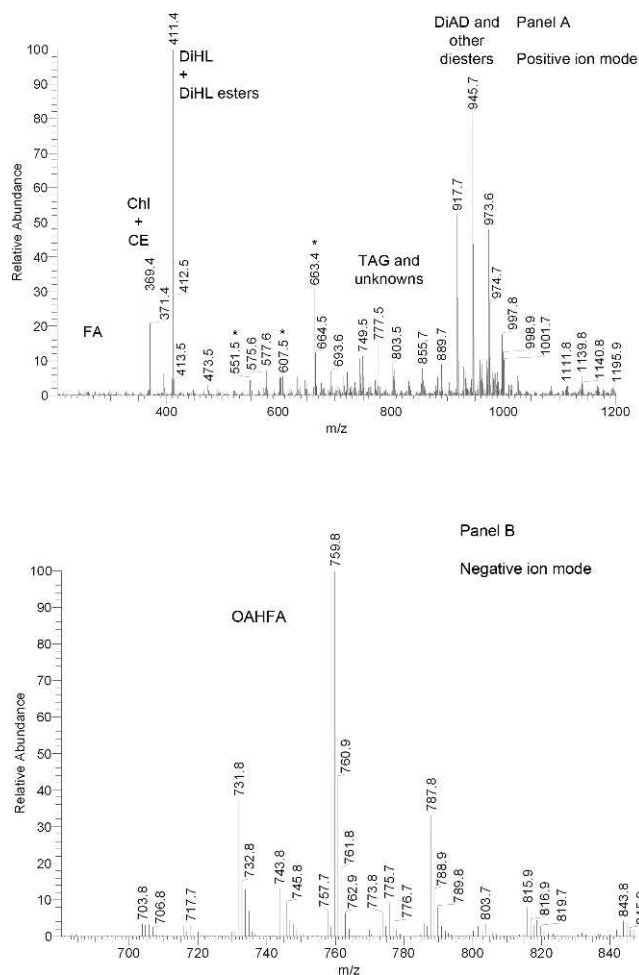
physiological one it was "oil-like" (Fig. 2B). The collected samples were treated and stored as described above for the human and mouse samples.

GLC/MS and HPLC/MS Experiments

MS, GLC/MS, and HPLC/MS experiments with all of the samples were conducted exactly as described below. Several techniques were employed. First, observation atmospheric pressure chemical ionization (APCI) MS spectra of a sample were recorded in both positive and negative ion modes using the direct injection approach. The samples were dissolved in $CHCl_3:CH_3OH$ equaling a 3:1 solvent mixture to make 0.1mg/mL stock solutions. Then, a 1 to 10 uL aliquot of sample solution was injected in the flow of an HPLC solvent (typically, a *n*-hexane:propan-2-ol:glacial acetic acid mixture [HPA; 95:4.9:0.1, vol/vol/vol]) and analyzed in the positive ion mode using the mass spectrometer with APCI ion source. Recorded spectra allowed us to assess the quality of the samples, and their suitability for subsequent, more rigorous, HPLC-style experiments. Then, the samples were analyzed for the presence of particular lipid classes, such as cholesterol (Chl) and cholesteryl esters (CE), (O-acyl)-ω-hydroxy fatty acids (OAHFA), WE, acyl glycerols (AG), ceramides (Cer), free FA, squalene (Sql), and other types of lipids, using previously tested HPLC/MS protocols. Briefly, the nonpolar lipids were analyzed using normal
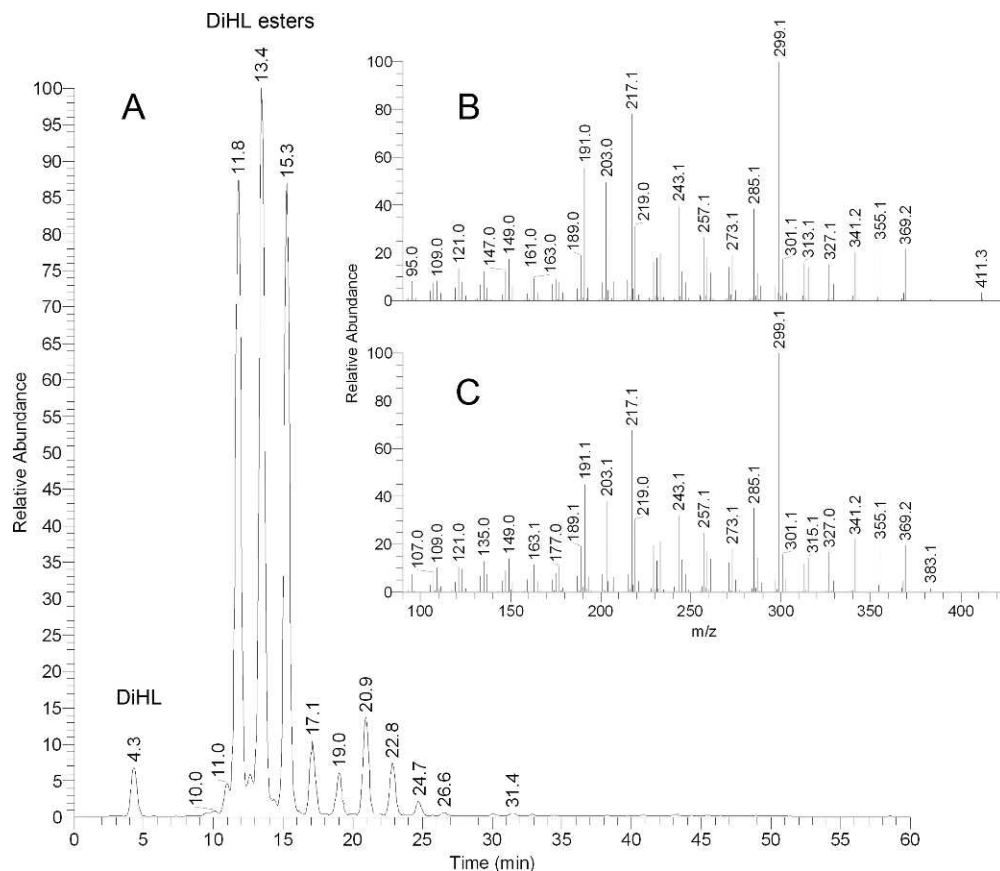
FIGURE 7. DiHL and its esters in rabbit meibum. The compounds were detected in the RP-HPLC experiment by monitoring ions with *m/z* values of 411 with subsequent fragmentation of the ions in MS/MS experiment with a collision-induced dissociation energy of 37 V. (**A**) Chromatogram of ion *m/z* 411 detected in rabbit meibum. (**B**) Fragmentation pattern of authentic DiHL. (**C**) Fragmentation pattern of a rabbit compound with *m/z* 411 with retention time of 13.4 minutes. Note that other peaks shown in (**A**) produced identical fragmentation spectra.

FIGURE 8.   Representative RP chromatograms of rabbit meibum. Ions *m/z* 411 (**A**), *m/z* 369 (**B**), and *m/z* 409 (**C**) were monitored. AA, peak area.

FIGURE 9. RP-HPLC/MS^n analysis of homologous compounds with m/z values of 889, 917, 945, and 973 found in rabbit meibum. (**A**) Extracted ion chromatograms of ions with m/z values of 889 (RT 20.5 minutes), 917 (22.3 minutes), 945 (24 minutes), and 973 (25.5 minu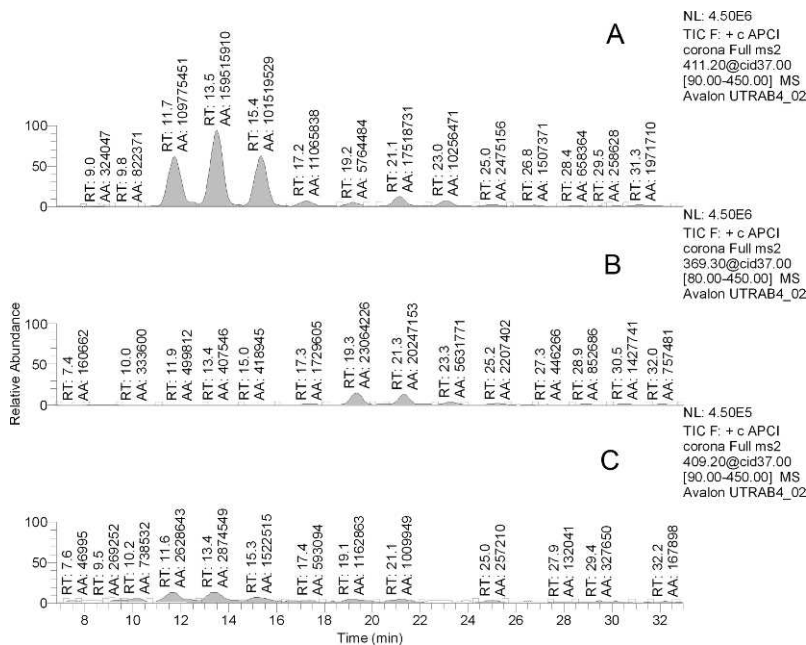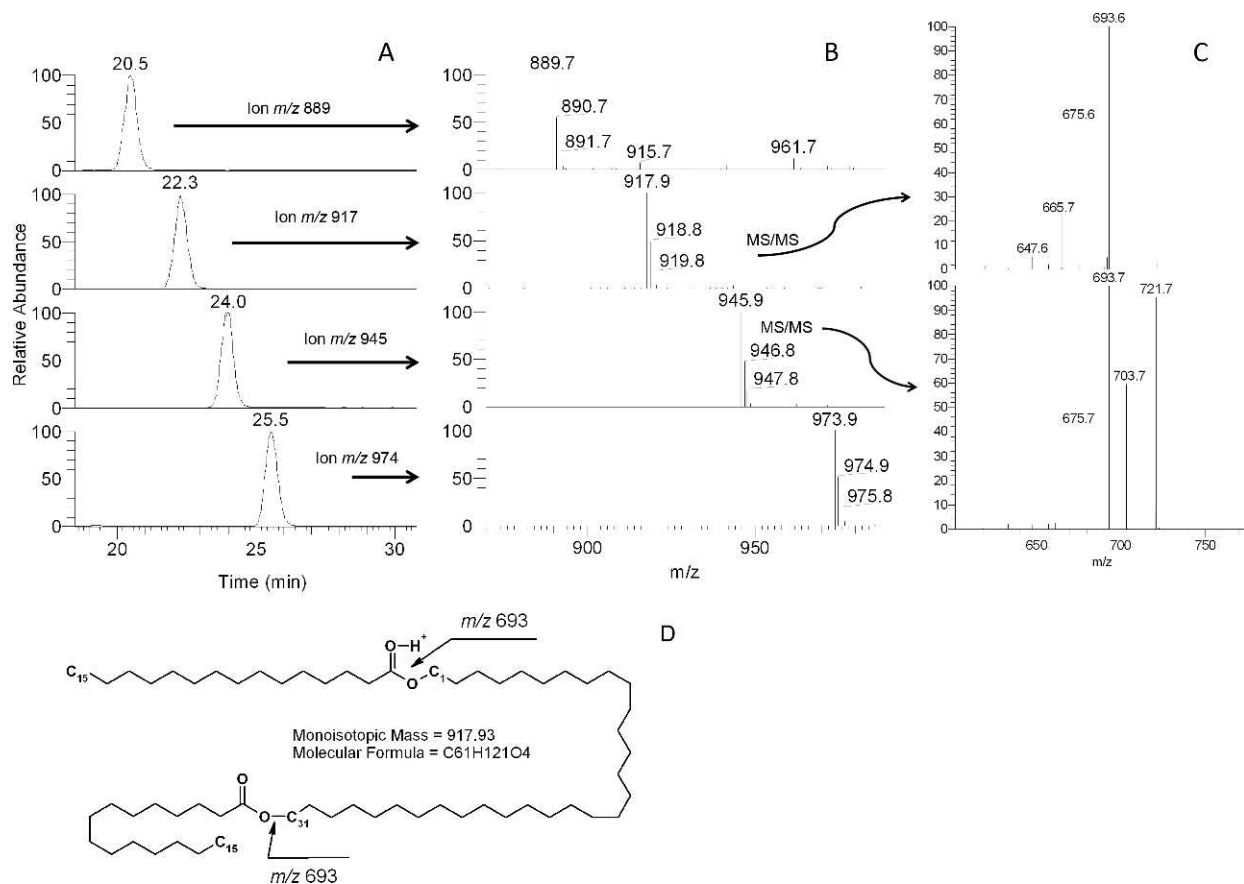tes). (**B**) Mass spectra of the HPLC peaks shown in (**A**). (**C**) MS/MS fragmentation spectra of ions m/z 917 and m/z 945. Note the presence of dehydrated product ions (such as m/z 675 [693 – H_2O] and 703 [721 – H_2O]) among the product ions. (**D**) Putative structure of compound m/z 917 (major isoform is shown; other isoforms may differ in the lengths of the diol and the FA moieties of the molecule with m/z 917).

phase (NP) and reversed phase (RP) HPLC and APCI MS, while more polar lipids were analyzed using NP/RP-HPLC and electrospray ionization (ESI) MS. For NP-HPLC experiments, a Diol silica gel column (3.1 × 150 mm, 5μm; Phenomenex, Torrance, CA) was used. The flow rate of the HPA solvent mixture was maintained at 0.3 mL/min. The column was equilibrated at 30°C. The RP-HPLC experiments were conducted using a Hypersil Gold C$_{18}$ silica gel column (2.1 × 150 mm, 5μm; ThermoFisher). Separation of analytes was achieved at 35°C using a gradient elution with a propan-2-ol:acetonitrile:0.2% aqueous acetic acid solvent mixture at a flow rate of 0.2mL/min as described earlier.[14] Most of the analytes (such as Chl, CE, Cer, free FA, OAHFA, Sql, WE) were analyzed using the APCI ion source.

The structures of individual lipids were determined in fragmentation MS/MS, and multistage mass spectrometry (MS^n with $n = 3$ and above requires an ion trap mass spectrometer) experiments as described earlier for WE, CE, OAHFA, and other lipids.[2,14,25,29–31] The ions of interest were isolated in the ion trap with an isolation width of 2 atomic mass unit (amu), and then fragmented at a collision-induced dissociation energy (CID) of 25 to 37 electron volts (eV). Where possible, the animal lipids were compared with authentic lipid standards, and with human lipids of the same types.
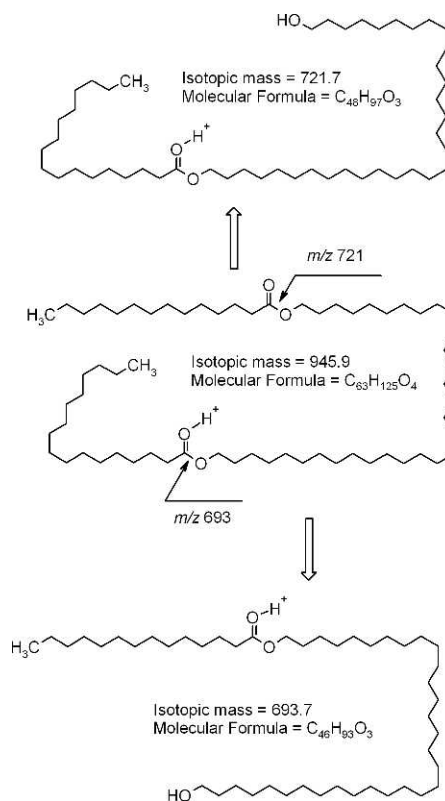

FIGURE 10. Fragmentation patterns of diacylated α,ω-diols. A major isoform of a mouse compound with m/z value of 945 is shown.
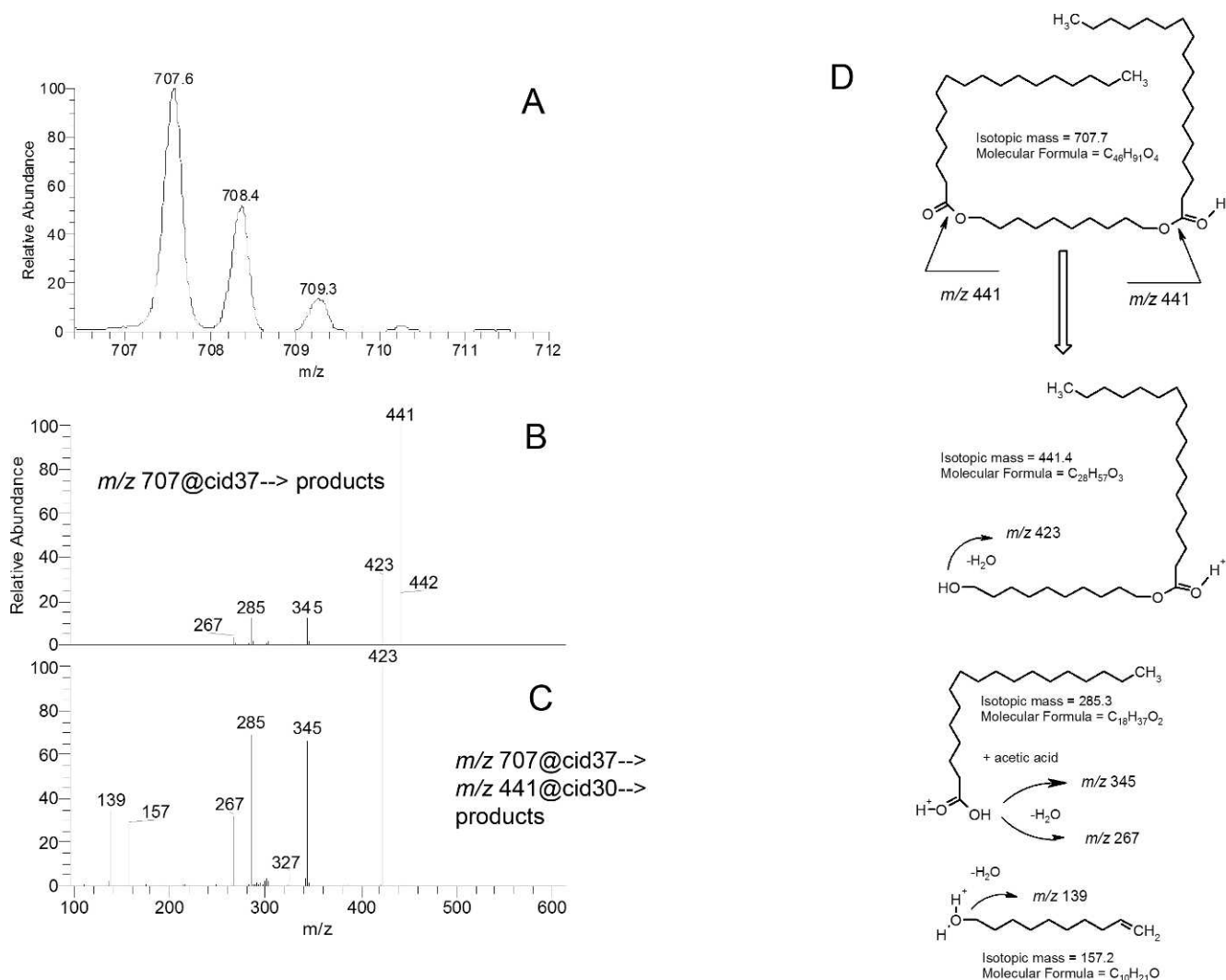
FIGURE 11. HPLC/MS/MS analyses of synthetic distearoyl-1,10-decanediol. (**A**) Mass spectrum of synthetic distearoyl-1,10-decanediol. (**B**) MS/MS analysis of ion *m/z* 707. (**C**) MS/MS/MS analysis of the product ion *m/z* 443. (**D**) Fragmentation pattern of synthetic distearoyl-1,10-decanediol.

Quantitation of lipids in HPLC/MS experiments was performed using calibration curves obtained with authentic lipid standards and corrected for the differences in the ionization efficiency as described earlier for CE.[30,31] In GLC/MS experiments, meibomian lipids were quantitated using 3 dimensional (3D mass-to-charge ratio [*m/z*] versus lipid sample weight versus signal intensity) calibration plots.[25]

The Mouse TFBUT

Analysis of TFBUT in mice was conducted using 2-month-old littermates as follows. To moderately sedate the mice and make it possible to measure their TFBUT under a surgery microscope (Möller-Wedel, Wedel, Germany), the animals were anesthetized with a ketamine (120 mg/kg) and xylazine (16mg/kg) cocktail. These experiments were proven to be all but impossible to conduct on fully active mice because of their agility. A procedure similar to the forced blinking procedure described by Nakamura et al.[32] was used. Sodium fluorescein (1 µL of a 1% solution in PBS) was applied to the lower conjunctiva sac, spread over the ocular surface by manually closing the animal's eyes three times, then opening the eye and timing until one or more black spots or streaks were recorded in the precorneal TF using a manual slit lamp with a cobalt blue filter (Kowa SL-2; Kowa, Nagoya, Japan). TFBUT measurements were recorded for four animals (eight eyes total). We attempted to evaluate corneas and conjunctivas in mice using slit-lamp evaluation and Lissamine green B staining[33] for any signs of ocular inflammation or other ocular abnormalities. However, strong pigmentation of the eyes of mice made it very difficult, if not impossible.

RESULTS

For the reader's convenience, structures of the compounds that will be discussed in this section are summarized in Figure 3. The GC-MS and HPLC-MS procedures used in this study have been validated and explained in detail in our preceding publications[2,14,25,30,31] (also see the references cited therein). Identification of meibomian lipids was conducted using several parameters, which included their *m/z* values, GC, and/or HPLC retention times, evaluation of fragmentation patterns of analytes in MS[n] experiments, and comparison of these parameters with those of authentic lipid standards. In lipid chemistry, the ability to perform sequential fragmentation of parent molecules (such as WE, OAHFA, etc.) is a critical factor that has been proven time and again to be an indispensible tool in unraveling structures of complex lipids and for discriminating between different isobaric compounds (i.e., compounds
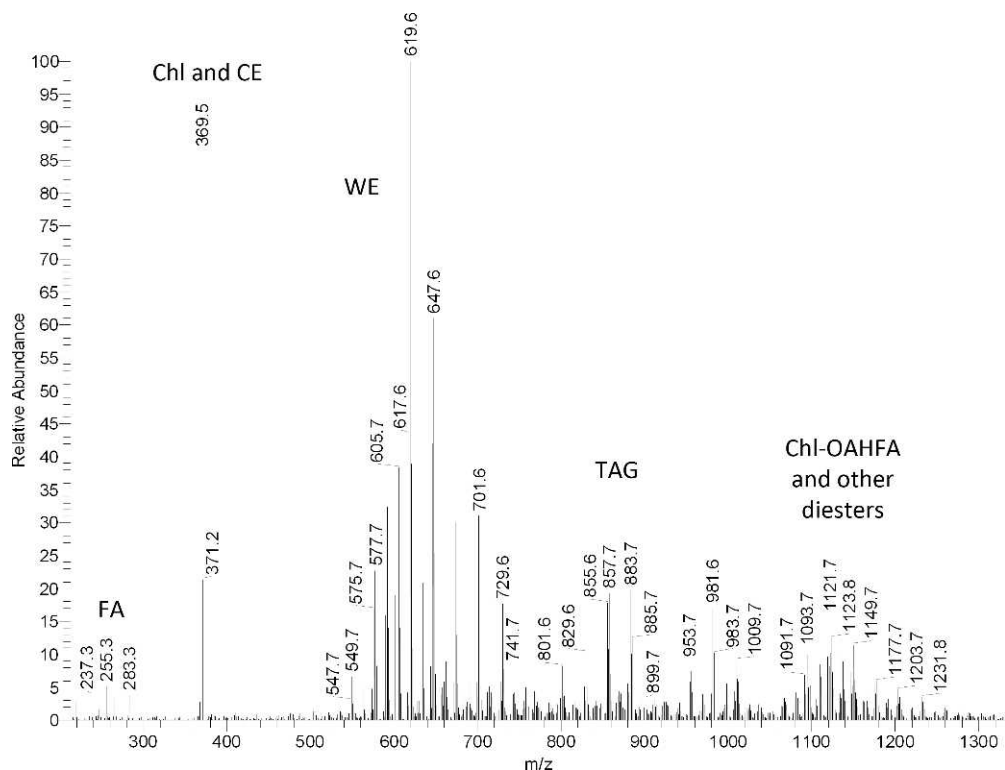
FIGURE 12. Representative mass spectra of mouse meibum. Positive ion mode atmospheric pressure chemical ionization mass spectrum.
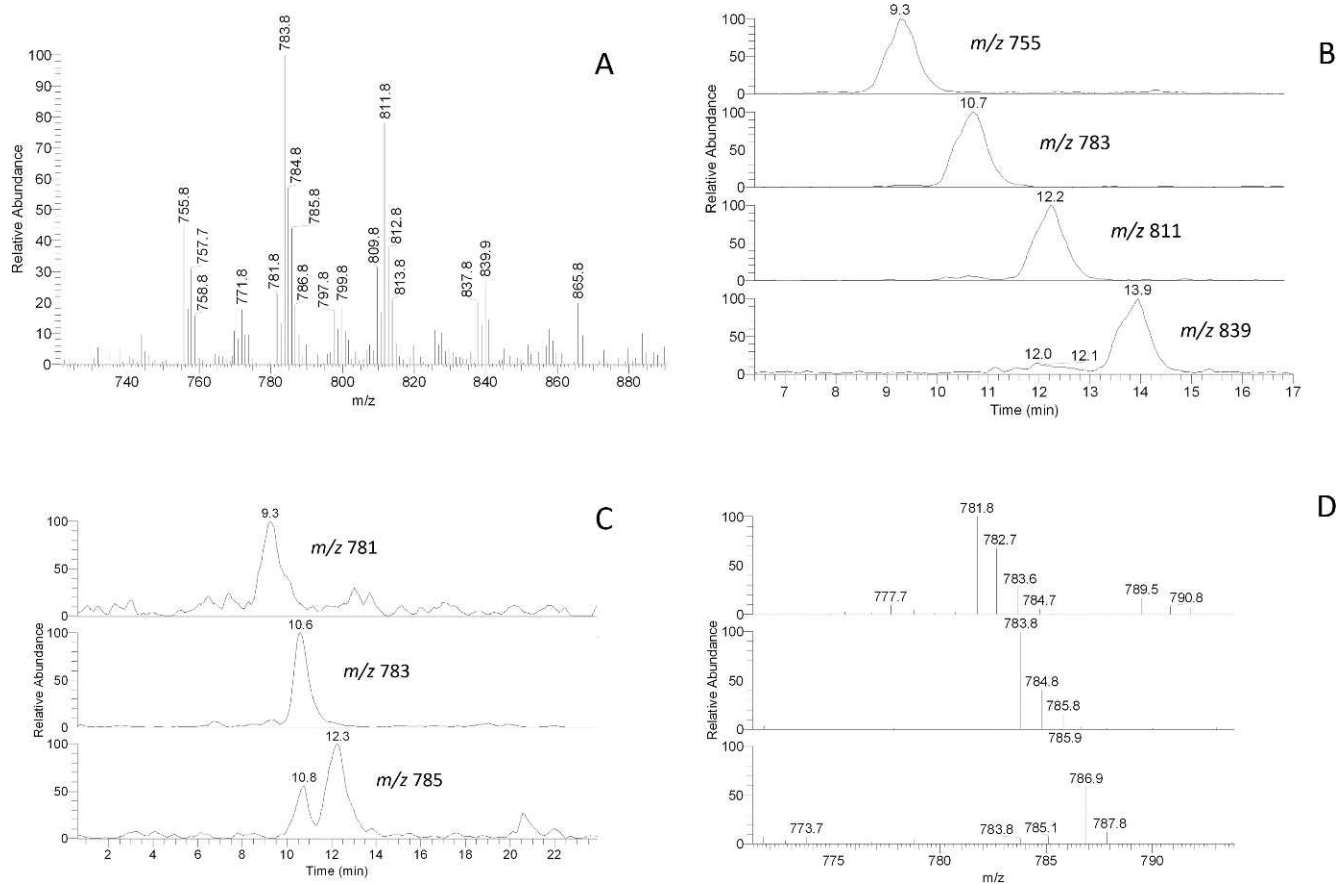
FIGURE 13. RP-HPLC/MS^n analysis of homologous OAHFA with *m/z* values of 755, 783, 811, and 839 found in mouse meibum. (**A**) Negative ion mode mass spectrum of the mouse OAHFA. (**B**) Extracted ion chromatograms of homologous ions *m/z* 755, 783, 811, and 839 differing by their carbon chain lengths. (**C**) Extracted ion chromatograms of homologous ions *m/z* 781, 783, and 785 differing by their degree of unsaturation. (**D**) Mass spectra of the HPLC peaks shown in (**C**).
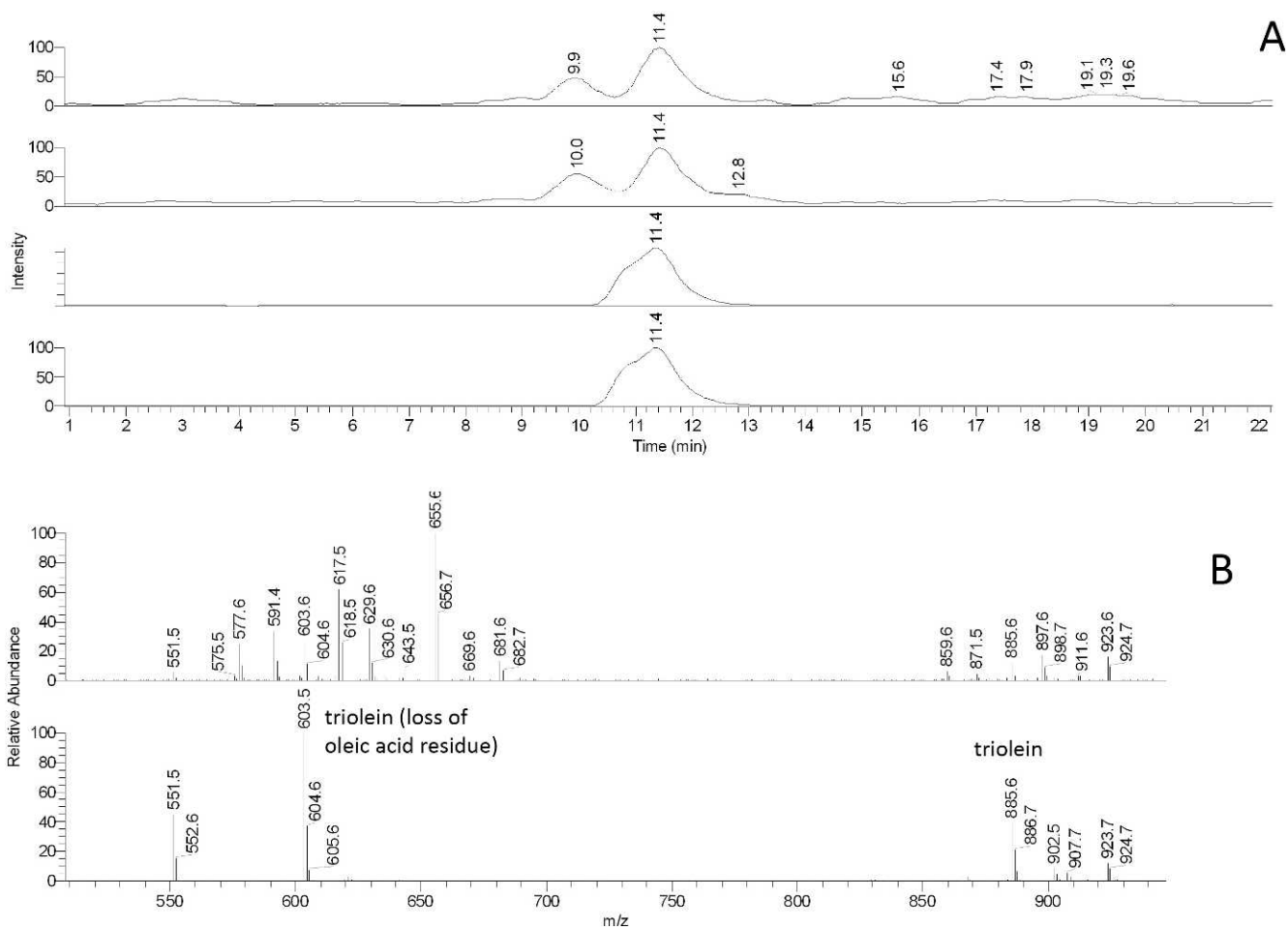
FIGURE 14. RP-HPLC/MS analysis of authentic triolein and isobaric triacylglycerols in mouse meibum. (**A**) Extracted chromatograms (from top to bottom) of ions m/z 885 (mouse), 603 (mouse), 885 (authentic triolein), and 603 (authentic triolein). (**B**) Mass spectra of the HPLC peaks shown in (**A**). *Upper spectrum*: mouse TAG. *Lower spectrum*: authentic triolein.

that have identical elemental composition, but different structures, such as positional, geometrical, and stereo-isomers with the same molecular formulas[25]). An alternative approach, using high accuracy mass spectrometers such as triple quadrupole, time-of-flight and magnetic sector instruments, is a capable alternative for verifying molecular masses of analytes, but is much less effective in dealing with isobaric compounds, and generally poorly suited for structural analyses of complex molecules as the vast majority of those instruments are either not capable of performing multiple sequential fragmentations essential for studying complex isobaric molecules, or extremely expensive and rare.

Mass spectra of human meibum (Fig. 4) recorded in the positive ion mode showed a typical distribution of MS signals, which were no different from those that had been reported before,[2,14,25,30,31] and had low interdonor variability.[25] Two low intensity ions with m/z values of 255 and 283 were clearly (M + H)$^+$ ions of $C_{16:1}$ (palmitoleic) and $C_{18:1}$ (oleic) acids, while related ions 265 and 237 were those of the dehydrated acids (M – H_2O + H)$^+$. The major MS signal in the spectra was invariably the one with m/z value of 369. It derived from two groups of lipids, Chl and CE, and was identified as a product ion of dehydrated Chl. Since no spatial separation of Chl and CE can be achieved in direct injection/direct infusion experiments, Chl and CE entered the MS detector simultaneously, and produced the same product ion m/z 369 through two different

in-source reactions, dehydration of free Chl (M – H_2O + H$^+$) and a neutral loss of FA residues by CE (M – FA + H$^+$), respectively. An ion m/z 383 (sometimes, but not always seen in the samples) has not been identified yet. A set of compounds with a common fragment m/z 411 was observed in positive ion mode (PIM) HPLC/APCI MS experiments. Their apparent abundances (estimated as HPLC peak areas of ion m/z 411) were approximately 4% of those of Chl and CE. An even smaller amount of compounds that produced a common ion m/z 409 was also detected. Similar compounds, but in much larger quantities, were observed in the rabbit samples (see below). A more detailed description of these lipids is provided later in the manuscript.

The largest group of signals with m/z values between 549 and 703 belonged to unsaturated WE. A group of signals with m/z values from 700 to 850 are those of OAHFA and CE. Though OAHFA are free acids, and are easier to detect in the negative ion mode (see below), they still form proton adducts of the (M + H)$^+$ type (much like the oleic and palmitoleic acids mentioned above), which makes them visible in the positive ion mode. CE, both of saturated and unsaturated types, produced a range of (M + H)$^+$ signals that corresponded to molecular formulas of $C_nH_{2n-9}O_2$, $C_nH_{2n-11}O_2$ and $C_nH_{2n-13}O_2$.

Another major group of ions (m/z 900–1200) are with all likelihood a very complex group of "diesters" that had originally been proposed by Nicolaides et al.[34] In human
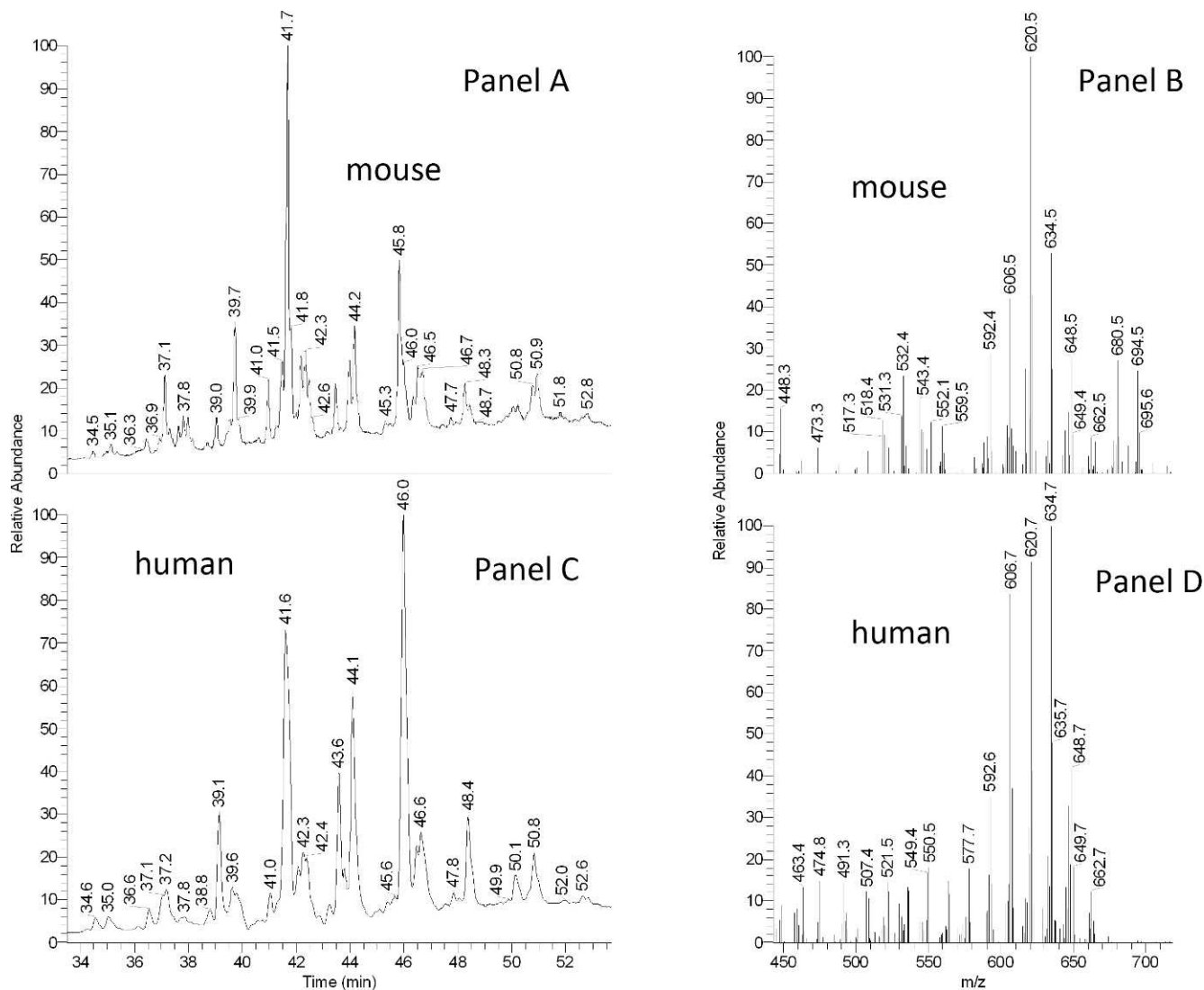
FIGURE 15. Comparative GLC/MS analysis of mouse and human meibum. (**A**) Total ion chromatograms of the WE region of the mouse meibum obtained using low voltage electron impact (EI) ion trap mass spectrometry. (**B**) Averaged mass spectrum of the GLC peaks shown in (**A**). (**C**) Total ion chromatograms of the WE region of the human meibum obtained using low voltage EI ion trap mass spectrometry. (**D**) An averaged mass spectrum of the GLC peaks shown in (**C**).

meibum, we observed ions m/z 1071, 1099, 1127, 1155, and 1183 that were previously found in canine meibum and identified as cholesteryl esters of OAHFA (Chl-OAHFA) with a general molecular formula of their $(M + H)^+$ ions $C_nH_{2n-16}O_4$ ($n = 73$ to 81).[14] A range of saturated and unsaturated α,ω-Type 2 diesters (FA-α,ωFDiol-FA) were also detected (Fig. 3).

The canine meibum, analyzed in the same conditions as the human samples, produced MS spectra that were very similar, though not identical, to the human ones (Fig. 5). Most noticeable were the qualitative differences in the relative intensities of WE and a larger presence of diester compounds with m/z values of 900 to 1050. When canine CE were evaluated, the same high degree of similarity with human meibum was observed. Molecular structures and relative abundances of canine OAHFA and Chl-OAHFA were indistinguishable from their human counterparts. Note that the triplet of ions m/z 663/607/551 was previously identified as an oxidized form of a common plasticizer Irgafos.[2]

On the other hand, rabbit meibomian lipids were found to be very different from human and canine samples (Fig. 6). Their complete characterization goes beyond the scope of this
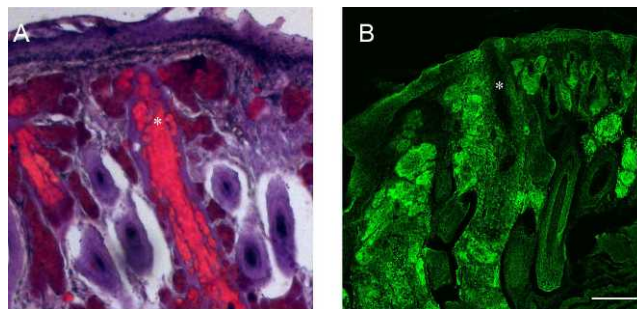
FIGURE 16. Lipid staining of mouse eyelids. (**A**) ORO staining lipid was detected throughout the meibomian ductile and ascinar system. In the central duct (*) ORO stained a large uninterrupted lipid mass but staining of more discrete masses was present in the inner ducts and ascini. (**B**) Confocal image using biotin-duramycin to stain eyelid PE. Staining outlines the periphery of cells in the epithelium, ascini, and hair shafts. Within the meibomian central ductal system the periphery of cells lining the duct are stained but no staining is detected within the central meibomian lipid containing region of the duct (*). *Scale bar* = 100 μm.

TABLE 1. Triacylglycerols of Mouse Meibum

m/z (M + H)$^+$	Molecular Formula	Total Number of Double Bonds/Molecule	m/z (M + H)$^+$	Molecular Formula	Total Number of Double Bonds/Molecule	m/z (M + H)$^+$	Molecular Formula	Total Number of Double Bonds/Molecule
825.5	$C_{53}H_{93}O_6$	5	837.5	$C_{54}H_{93}O_6$	6	851.6	$C_{55}H_{95}O_6$	6
827.5*	$C_{53}H_{95}O_6$	4	839.6*	$C_{54}H_{95}O_6$	5	853.6	$C_{55}H_{97}O_6$	5
829.6*	$C_{53}H_{97}O_6$	3	841.5*	$C_{54}H_{97}O_6$	4	855.6*	$C_{55}H_{99}O_6$	4
831.5	$C_{53}H_{99}O_6$	2	843.5	$C_{54}H_{99}O_6$	3	857.6*	$C_{55}H_{101}O_6$	3
865.5	$C_{56}H_{109}O_6$	6	879.6	$C_{57}H_{99}O_6$	6	891.6	$C_{58}H_{99}O_6$	7
867.5*	$C_{56}H_{107}O_6$	5	881.6*	$C_{57}H_{101}O_6$	5	893.6	$C_{58}H_{101}O_6$	6
869.5*	$C_{56}H_{105}O_6$	4	883.6*	$C_{57}H_{103}O_6$	4	895.5*	$C_{58}H_{103}O_6$	5
871.6	$C_{56}H_{103}O_6$	3	885.6	$C_{57}H_{105}O_6$	3	897.6	$C_{58}H_{105}O_6$	4

* Major lipid species.

paper. Nevertheless, a few comments are warranted. The most prominent peak in the PIM spectra was the one with m/z value of 411. In human samples, this (extremely minor) peak was putatively identified as Sql[2]: under the conditions of NP-HPLC it coeluted with authentic standard, and their MS/MS fragmentation patterns matched. However, in RP-HPLC experiments with human samples, a series of at least 10 minor compounds that produced ion m/z 411 was discovered. Their retention times (RT) ranged from 4.5 to 25 minutes. Conversely, when rabbit samples were analyzed using RP-HPLC, this ion produced at least 10 major HPLC peaks with RT differing from 4.4 to almost 25 minutes (Fig. 7A). An important HPLC peak of this ion had a RT of 4.3 minutes, which was very close, but slightly longer that the RT of free Chl (4.2 minutes). Interestingly, the other three major HPLC peaks of ion m/z 411 with RT of approximately 12, 13, and 15 minutes coeluted with three compounds whose m/z values were 803, 831, and 859, respectively (not shown). Thus, ion m/z 411 with the shortest RT of 4.3 minutes was most likely produced by a free compound, while the analytes with longer RP-HPLC retention times were with all likelihood its more complex and hydrophobic derivatives. Importantly, its fragmentation pattern did not match that of authentic Sql, confirming that the rabbit compound was of a different nature. However, its fragmentation resembled that of Chl. Therefore, it seemed that the compound m/z 411 was of a sterol nature, and was a product ion of the same in-source dehydration reaction that leads to m/z 386-to-m/z 369 transformation typical of Chl. This implied that ion m/z 411 was of (M – H$_2$O + H)$^+$ type. The only common mammalian sterol that has a molecular weight of 428 is 24,25-dihydro-Δ^8-lanosterol (DiHL). Its presence in rabbit meibum was initially proposed by Tiffany et al.[20] To determine whether the rabbit compounds (both the free sterol and its esters) were indeed DiHL-related, their fragmentation patterns were compared with one of authentic DiHL and found to be similar (Figs. 7B, 7C). Thus, it became clear that DiHL was present in rabbit meibum as a free sterol as well as its esters with extremely long chain FA (ELCFA). Three detected ions with m/z values of 803, 831, and 859 were, apparently, those of DiHL esters of $C_{26:2}$, $C_{28:2}$, and $C_{30:2}$ ELCFA. To the best of our knowledge, none of these esters had been previously described for any animals or humans. A minor presence of free and esterified dehydrolanosterol (DeHL; characteristic ion m/z 409, [M-H$_2$O+H]$^+$) was also observed. Again, its fragmentation pattern and RT of free compound replicated those of authentic DeHL (not shown).

Judging from chromatograms of their corresponding analytical ions (Fig. 8), the abundances of the rabbit Chl-containing compounds were less than or equal to 10% of those

based on DiHL, while DeHL-based compounds were between 1% and 2% of their DiHL counterparts.

Other major compounds detected in the rabbit meibum included ions m/z 889, 917, 945, and 973. Their fragmentation patters (Figs. 9, 10) provided strong evidences that they were di-acylated diols (DiAD). To confirm this hypothesis, two model lipids of the same nature, distearoyl-1,10-decanediol and 1,10-dioleoyl-decanediol, were made through the reaction of acylation of 1,10-decanediol with either stearoyl chloride or oleoyl chloride (fatty acid chlorides are known to readily react with alcohols in the presence of a suitable catalyst[35]). These model compounds were shorter than their natural homologs, but their fragmentation appeared to proceed in the same fashion (Fig. 11; only saturated lipid is shown; the characteristic ions of doubly unsaturated DiAD were two units lighter than those of the saturated one). The model compounds were detected as (M + H)$^+$ ions that, apparently, were quite stable and did not undergo any spontaneous in-source fragmentation that is characteristic of some other groups of lipids such as CE and triacylglycerol (TAG). Importantly, another group of lipids that could produce similar ions, etherdiesters with the general formulas $C_nH_{2n-1}O_5$ (saturated), $C_nH_{2n-3}O_5$ (monounsaturated), $C_nH_{2n-5}O_5$ (diunsaturated), and so on, did undergo spontaneous in-source fragmentation, and were seen mostly as (M – fatty acid + H)$^+$ ions.

The highest degree of similarity with human meibum was observed for the mouse meibomian gland secretions. First, its observation mass spectrum taken in positive ion mode during a NP-HPLC experiment (Fig. 12) showed a distribution of signals of Chl/CE (m/z 369) and WE (m/z 549-729) almost identical to that of human meibum (Fig. 4). A group of ions with m/z values between 700 and 850 were found to be a complex mixture of CE and TAG. A range of compounds with m/z values between 950 and 1200 were of the diester nature. The groups of TAG and diesters were elevated compared with human samples, but were very close structure wise. The last group of detected compounds (m/z 900–1200) with retention times between 25 and 35 minutes (Fig. 8B) was similar to canine and human Chl-OAHFA.[14] The structural assignments of Chl, CE, WE, TAG, and Chl-OAHFA were confirmed in fragmentation experiments. Similarly to human WE, the mouse WE were based primarily on three unsaturated FA ($C_{16:1}$, $C_{18:1}$, and $C_{18:2}$), several saturated FA ($C_{15:0}$ to $C_{20:0}$), and a range of long chain fatty alcohols (FAl) with varying chain lengths. The latter were either observed as FAl product ions, or calculated as difference between the (M + H)$^+$ ions of WE and their FA fragments. The CE group was comprised of compounds based on fatty acids ranging from $C_{16:1}$ to $C_{28:0}$.

In negative ion mode, the spectra also closely resembled the spectra of human samples: the most prominent signals (Fig. 13)

TABLE 2. OAHFA in Human and Animal Meibum

Measured m/z $(M - H)^-$	Molecular Formula $(M - H)^-$	Total Number of Double Bonds/Molecule	Theoretical m/z $(M - H)^-$
Human OAHFA			
701.8	$C_{46}H_{85}O_4$	2	701.6
703.8	$C_{46}H_{87}O_4$	1	703.7
729.8*	$C_{48}H_{89}O_4$	2	729.7
731.9‡	$C_{48}H_{91}O_4$	1	731.7
743.8‡	$C_{49}H_{91}O_4$	2	743.7
745.8‡	$C_{49}H_{93}O_4$	1	745.7
755.7†	$C_{50}H_{91}O_4$	3	755.7
757.9*	$C_{50}H_{93}O_4$	2	757.7
781.7‡	$C_{52}H_{93}O_4$	3	781.7
783.8*	$C_{52}H_{95}O_4$	3	783.7
785.8†	$C_{52}H_{97}O_4$	2	785.7
Mouse OAHFA			
701.7‡	$C_{46}H_{85}O_4$	2	701.6
703.7‡	$C_{46}H_{87}O_4$	1	703.7
729.8†	$C_{48}H_{89}O_4$	2	729.7
731.9‡	$C_{48}H_{91}O_4$	1	731.7
743.8‡	$C_{49}H_{91}O_4$	2	743.7
745.9‡	$C_{49}H_{93}O_4$	1	745.7
755.8†	$C_{50}H_{91}O_4$	3	755.7
757.9†	$C_{50}H_{93}O_4$	2	757.7
781.8	$C_{52}H_{93}O_4$	4	781.7
783.9*	$C_{52}H_{95}O_4$	3	783.7
785.9†	$C_{52}H_{97}O_4$	2	785.7
797.8‡	$C_{53}H_{97}O_4$	3	797.7
799.9‡	$C_{53}H_{99}O_4$	2	799.7
809.9†	$C_{54}H_{97}O_4$	3	809.7
811.9*	$C_{54}H_{99}O_4$	2	811.8
827.7‡	$C_{55}H_{103}O_4$	2	827.8
829.8‡	$C_{55}H_{105}O_4$	1	829.8
Canine OAHFA			
701.7‡	$C_{46}H_{85}O_4$	2	701.6
703.7‡	$C_{46}H_{87}O_4$	1	703.7
715.7‡	$C_{47}H_{87}O_4$	2	715.7
717.7‡	$C_{47}H_{89}O_4$	1	717.7
729.8*	$C_{48}H_{89}O_4$	2	729.7
731.9‡	$C_{48}H_{91}O_4$	1	731.7
743.8‡	$C_{49}H_{91}O_4$	2	743.7
745.8‡	$C_{49}H_{93}O_4$	1	745.7
755.7	$C_{50}H_{91}O_4$	3	755.7
757.8*	$C_{50}H_{93}O_4$	2	757.7
781.7‡	$C_{52}H_{93}O_4$	3	781.7
783.8‡	$C_{52}H_{95}O_4$	3	783.7
785.8†	$C_{52}H_{97}O_4$	2	785.7
Rabbit OAHFA			
703.8‡	$C_{46}H_{87}O_4$	1	703.7
705.8‡	$C_{46}H_{87}O_4$	1	703.7
715.7‡	$C_{47}H_{87}O_4$	2	715.7
717.7‡	$C_{47}H_{89}O_4$	1	717.7
731.9†	$C_{48}H_{91}O_4$	1	731.7
733.9	$C_{48}H_{93}O_4$	0	733.7
743.8‡	$C_{49}H_{91}O_4$	2	743.7
745.9‡	$C_{49}H_{93}O_4$	1	745.7
757.8‡	$C_{50}H_{93}O_4$	2	757.7
759.9*	$C_{50}H_{95}O_4$	1	759.7
785.7‡	$C_{52}H_{97}O_4$	2	785.7
787.9*	$C_{52}H_{96}O_4$	1	787.7
815.9‡	$C_{54}H_{101}O_4$	1	813.8

Compounds were detected using the negative ion mode HPLC/MS protocol.

The analytes were semi-quantified as follows with the unmarked values as average peak(s):

    * Major peak(s);

    † Prominent peak(s);

    ‡ Minor peak(s).

were identical with those of mono-, di-, and tri-unsaturated OAHFA characterized in previous experiments with human and canine meibum[14] (and references cited therein). The mouse compounds were studied in fragmentation HPLC/MS^n experiments and were shown to be based on a mixture of $C_{16:n}$, $C_{17:n}$, and $C_{18:n}$ FA ranging from n equals 0 to n equals 2: note the regular pattern of homologous HPLC peaks differing by either a number of carbons (Figs. 13A, 13B), or by degree of unsaturation (Figs. 13C, 13D). It became evident that most of the OAHFA species were of an unsaturated nature.

Similarly to humans and opposite to rabbits, mice had only a minor presence of DeHL- and DiHL-based compounds: the relative amount of CE in the mouse meibum was approximately 30 times higher than that of DiHL-based esters. Interestingly, canines had no detectable amounts of lanosterol-related lipids in their meibum as no HPLC/MS peaks of ions with values of m/z 411 were detected above the noise level.

Another group of lipids that is prominently present in rabbits, and to a lesser extent in canines, DiAD with m/z values of 889, 917, 945, and 973, were not detected in human or mouse meibum in appreciable quantities. However, a range of tentatively similar compounds with a higher degree of unsaturation (e.g., groups of lipids with m/z values of 951/953/955, 965/967/969, and 979/981/983) were indeed detected. Considering the high complexity of this group of esters, their structures will be reported in subsequent publications.

As mice reportedly have TAG in their meibum,[16] the mouse samples were evaluated for these compounds using an approach illustrated in Figure 14 for triolein. Triolein itself produced a noticeable $(M + H)^+$ peak with m/z value of 885. However, the compound underwent strong spontaneous in-source fragmentation giving another characteristic ion m/z 603 $[(M - \text{oleic acid} + H)^+]$. Both ions coeluted with the same ions produced by authentic triolein. The mouse TAGs were found to be a very complex mixture of various combinations of saturated and unsaturated FA. The number of all possible TAGs generated from n various FA is n^3 (e.g., see a paper by Small[36]). Thus, even a modest three FA can lead to 27 possible TAGs, which made a comprehensive analysis of TAGs impractical at this time. However, our preliminary data on these species are summarized in Table 1. Importantly, tested samples of human meibum also had (albeit smaller) amounts of TAG, for example triolein, in its composition.

GLC/MS analysis of WE of mouse meibum (Fig. 15) was performed as described earlier for human meibum.[25] Again, the human and the mouse samples were found to be qualitatively similar: WE of mice were demonstrated to be of almost identical molecular masses (between 550 and 650) and be based on a mixture of C_{16}, C_{17} and C_{18}-FA with various degrees of unsaturation. Finally, no noticeable correlation between the sex and the lipid composition of meibum was observed for either humans or mice. We expect this possibility to be explored in the future in more detailed studies with larger number of subjects.

To evaluate how meibum was distributed within the mouse meibomian glands, eyelids were surgically removed from euthanized animals, and stained with specific stains. Generally, meibomian glands in mice are aligned along the full extent of the inner surface of both the upper and lower eyelids and the orifice of these glands are visible on the eyelid margins as spots against the pigmented lid margins. Mouse eyes, similarly to those of guinea pigs,[37] contain two subconjunctival sebaceous glands located in the temporal aspect of the eyes. In this study, eyelid flaps were dissected to exclude analysis of secretions from these glands. Since the surface area of the eyelid margin in mice is both small and close to the animals fur, expression was performed in euthanized mice where with a lower temperature the lipid secretions emerged and remained on

TABLE 3. Lipid Composition of Meibum of Tested Animals and Humans

	Species			
Lipid Class	Humans	Mice	Canines	Rabbits
WE	Major (40%)	Major	Major	Traces
Chl	Low (<0.5%)	Low	Low	Low
CE	Major (30%)	Major	Major	Low
DiHL	Traces	Traces	Traces	Low
DiHL esters	Traces	Traces	Traces	Major
TAG	Low	Low	Low	Low
DAG	N/D	Low/traces	Low/traces	Low/traces
DiAD	Low	Low	Low	Major
OAHFA	Major amphiphiles	Major amphiphiles	Major amphiphiles	Major amphiphiles
Chl-OAHFA	Moderate	Moderate	Moderate	Traces
Squalene	Traces	Low	Low	Low
Ceramides	Traces	Low	Traces	Traces
Phospholipids and sphingomyelins*	Low (<0.1%)	Traces	Traces	Traces
Hydrocarbons†	N/D	N/A	N/A	N/A

For the lack of necessary lipid standards, compounds were evaluated using the following semi-quantitative scale: N/D < traces < low < moderate < major. Quantitative data are included where available. N/D, not detected; N/A, data not available.

* Analyzed by HPLC-ESI MS as described earlier.[48]

† Analyzed by GLC/MS.

the eyelid margin surface, rather than emerging as a clear liquid secretion as see in normal human meibum collections. Examination of mouse eyelids with ORO staining showed that within the meibomian glands lipid was present throughout the full extent of the ductile system, both the main duct and those ducts coming from the acini (Fig. 16A). Lipid stain was also present in the gland acini. The stained material in the main duct appeared as a uniform uninterrupted lipid mass whereas in the acini the staining was visible as more discrete staining entities, possibly representing staining of large fat droplets within developing acinar cells.

Staining of mouse eyelids with the tetracycline peptide, duramycin, which binds specifically to phosphatidyl ethanolamine (PE), showed abundant staining outlining the periphery of cells in multiple eyelid structures, including within the epidermis, in the meibomian acini and in cells lining the central duct of the meibomian glands (Fig. 16B). Such staining most likely represent plasma membrane localized PE. Notably absent from the duramycin staining is, however, any staining of the material localized within the region of the central meibomian duct.

Finally, the mouse TFBUT was measured and determined to be in the range between 3 and 6 seconds (on average, 5 ± 1 second, mean ± SD).

DISCUSSION

Our comparative studies led us to a conclusion that rabbit meibum was too different from the human one to be considered a valid animal model of human meibomian gland secretions, at least from the biochemical standpoint. The large quantities of DiAD and DiHL-containing esters and the low quantities of WE, Chl, and CE in rabbits set this species apart from the other tested animals. In view of these profound differences between the meibomian lipidomes of humans and rabbits, a better animal model for future studies of the biochemistry, biophysics, and physiology of meibum and the TF was needed: one can hardly expect that the metabolic and signaling pathways, regulatory mechanisms, and mechanisms of stabilization of the TF are the same for two such different organisms.

Mice, on the other hand, were biochemically close to the humans, as were canines (noted were the close similarities in the makeup of pools of WE, CE, OAHFA, and Chl-OAHFA). Considering that (1) the mouse genome, biochemistry, and physiology have been extensively studied and documented, (2) multiple gene knock-in and knock-out lines of mice have been generated, (3) the life cycle of mice is much shorter than that of canines, and (4) the maintenance costs for colonies of rodents are much lower, mice seem to be a better choice for experimental work with meibum and the TF. Canines, however, could be used in less invasive experiments, or when larger amounts of meibum and tears are needed. Additionally, some breeds of canines, such as spaniels, terriers, Lhasa Apso, and Shih-Tzu, among others,[38-40] are prone to dry eye, need to be treated for this condition, and can possibly be used as a natural model of humans with the same disease. As the relative intensities of signals with *m/z* of 369 (Chl + CE) and the group of WE is very similar for humans, canines, and mice, one can predict that the overall molar ratios of these compounds in the three species will be found to be close, too. However, individual variations within lipid classes (especially with regard to their structural isomerism,[14] are to be evaluated in future experiments.

An important factor to consider is the presence or absence of amphiphilic lipids in meibum. This very diverse group of lipids is believed to be critically important for efficient spreading of meibum on the ocular surface and forming the TFLL. Earlier, a novel group of amphiphilic lipids, extremely long chain OAHFA, was discovered in human[41] and canine[14] meibum. It was important to determine whether OAHFA are present in other animal species as well. Therefore, we evaluated the mouse meibum for the presence of OAHFA and did indeed observe these compounds in tested samples (Fig. 13). A list of the mouse OAHFA is presented in Table 2. Again, striking similarities between the human and the mouse lipids were observed: most of the OAHFA detected in humans were also observed in mice. However, the mice had a few more OAHFA homologs, most notably ions *m/z* 809.9, 811.9, and 837.9, which were two to four carbon atoms longer than typical human OAHFA. Interestingly, rabbit meibum also has OAHFA of almost exactly the same length, but of reproducibly higher degree of saturation: note that the most prominent

representatives of this class in rabbits, ions *m/z* 759.9 and 787.9, are 2 mass units heavier than the most common OAHFA found in humans and mice. This observation confirms that OAHFA are present in five out of five tested species (humans, mice, canines, and rabbits compared in this paper, and in the *Gorilla gorilla*, as described earlier [Wojtowicz JC, et al. *IOVS* 2010;51:ARVO E-Abstract 4160]).

Thus, our HPLC/MS and GLC/MS data left little doubt that, among animal species that can be used in routine laboratory experiments (excluding *Gorilla gorilla*), the mouse meibomian lipidome was the most similar to the human one, while the canine meibum was a close second (Table 3).

Two other important factors to consider are the TFBUT and the blinking rate. Being physiologically significant parameters, the TFBUT and the blinking rate are correlated with the stability of the TF. Rabbits blink very seldom (reportedly, once every 20 minutes or so[42]), and their TFBUT is extremely long, definitely longer than 30 seconds.[43] Considering these facts, and the vast differences between the meibomian lipidomes of rabbits and humans reported in this paper, the rabbit, from our standpoint, should not be used as a model for the human TF and meibum studies, especially those concerned with their biochemistry and biophysics.

The blinking rate in canines (approximately 8 seconds in puppies, and 25–30 seconds in adult dogs) is much closer to that in humans, while TFBUT in canines was measured to be just under 20 seconds.[44] Together with demonstrated similarities in the human and canine meibomian lipidomes, these observations make dogs attractive candidates for detailed meibum and TF studies.

Mice blink infrequently,[45] and the mechanism, through which their meibum is secreted onto the ocular surface, to the best of our knowledge, is not understood. It seems plausible that, instead of active spreading of meibum by moving (closing and opening) eyelids, mice rely on either passive spreading of meibum excreted by the glands, or on eyeball movements that can achieve the same effect. However, their TFBUT was measured in our experiments to be a reasonable 5 ± 1 second.

Another advantage of using mice is the anatomical similarities in the meibomian glands of mice and humans,[46,47] In both species individual meibomian glands have a central duct with an orifice that opens onto the eyelid surface, and connected to the central duct by small ductile are the meibomian holocrine secretory ascini. Within each ascinus, meibocytes undergo differentiation as they move from the periphery towards the center where they disintegrate and release their lipid products.[6] Lipid-specific staining with ORO and duramycin demonstrated that the meibum of mice is produced and excreted essentially as described for humans. Note the absence of the phospholipid-specific staining in the lipid mass accumulated in the central meibomian duct (Fig. 16) which corroborates results of our MS experiments where no noticeable signals of phospholipids (such as PE, SM, and PC) were observed. Nevertheless, we expect these compounds to be present in meibum, albeit in very low quantities, which are unlikely to play any structural role in the tear film in general and in its lipid layer specifically. In our previous studies phospholipids (such as phosphatidylcholine) were observed in meibum in quantities of less than or equal to 0.05% (i.e., 1 molecule of phosphatidylcholine per ~2,000 molecules of other lipids, or 500 parts per million [ppm]),[48] while in a recent report[49] the amounts of phospholipids in tears were estimated to be even smaller 1 ppm or less, with the major lipid detected, phosphatidylcholine, to be present in the amounts of less than or equal to 0.2 ppm. Considering the results published by Georgiev et al.[50] who demonstrated that to have a significant effect on the biophysical properties of MLF, phospholipids have to be present in the amounts 0.2

molar parts (i.e., 200,000 ppm) or more, the impact of the tiny amounts of phospholipids observed in our earlier experiments[48] and in a recent paper[49] on the properties of meibomian lipid films is expected to be minor. Finally, interdonor variability of meibum was re-evaluated and shown to be very small. This observation was in line with our previous reports.[2,14,25,30,31,48] Other questions related to the possible effects of age, diet, sex, environment, etc. were beyond the scope of this study. We expect these, and other, important subjects to be addressed in future publications on the topic.

References

1. Wolkoff P. Ocular discomfort by environmental and personal risk factors altering the precorneal tear film. *Toxicol Lett*. 2010;199:203–212.

2. Butovich IA. On the lipid composition of human meibum and tears: comparative analysis of nonpolar lipids. *Invest Ophthalmol Vis Sci*. 2008;49:3779–3789.

3. Dean AW, Glasgow BJ. Mass spectrometric identification of phospholipids in human tears and tear lipocalin. *Invest Ophthalmol Vis Sci*. 2012;53:1773–1782.

4. Rantamäki AH, Seppänen-Laakso T, Oresic M, Jauhiainen M, Holopainen JM. Human tear fluid lipidome: from composition to function. *PLoS One*. 2011;6:e19553.

5. Meibom, H. De vasis palpebrarum novis epistolae. Helmstadt, H. Muller; 1666.

6. Knop N, Knop E. Meibomian glands. Part I: anatomy, embryology and histology of the meibomian glands [in German]. *Ophthalmologe*. 2009;106:872–883.

7. Nicolaides N, Kaitaranta JK, Rawdah TN, Macy JI, Boswell FM III, Smith RE. Meibomian gland studies: comparison of steer and human lipids. *Invest Ophthalmol Vis Sci*. 1981;20:522–536.

8. McCulley JP, Sciallis GF. Meibomian keratoconjunctivitis. *Am J Ophthalmol*. 1977;84:788–793.

9. Tiffany JM. The role of meibomian secretion in the tears. *Trans Ophthalmol Soc U K*. 1985;104:396–401.

10. Mathers WD, Lane JA. Meibomian gland lipids, evaporation, and tear film stability. *Adv Exp Med Biol*. 1998;438:349–360.

11. Holly FJ. Physical chemistry of the normal and disordered tear film. *Trans Ophthalmol Soc U K*. 1985;104:374–380.

12. Kaercher T, Bron AJ. Classification and diagnosis of dry eye. *Dev Ophthalmol*. 2008;41:36–53.

13. Holly FJ, Lemp MA. Tear physiology and dry eyes. *Surv Ophthalmol*. 1977;22:69–87.

14. Butovich IA, Borowiak AM, Eule JC. Comparative HPLC-MS analysis of canine and human meibomian lipidomes: many similarities, a few differences. *Sci Rep*. 2011;1:24.

15. Harvey DJ, Tiffany JM. Identification of meibomian gland lipids by gas chromatography-mass spectrometry: application to the meibomian lipids of the mouse. *J Chromatogr*. 1984;301:173–187.

16. Miyazaki M, Man WC, Ntambi JM. Targeted disruption of stearoyl-CoA desaturase1 gene in mice causes atrophy of sebaceous and meibomian glands and depletion of wax esters in the eyelid. *J Nutr*. 2001;131:2260–2268.

17. Greiner JV, Glonek T, Korb DR, Booth R, Leahy CD. Phospholipids in meibomian gland secretion. *Ophthalmic Res*. 1996;28:44–49.

18. Harvey DJ. Identification by gas chromatography/mass spectrometry of long-chain fatty acids and alcohols from hamster meibomian glands using picolinyl and nicotinate derivatives. *Biomed Chromatogr*. 1989;3:251–254.

19. Tiffany JM. The meibomian lipids of the rabbit. I. Overall composition. *Exp Eye Res*. 1979;29:195–202.

20. Tiffany JM, Marsden RG. The meibomian lipids of the rabbit. II. Detailed composition of the principal esters. *Exp Eye Res*. 1982;34:601–608.

21. Harvey DJ, Tiffany JM, Duerden JM, Pandher KS, Mengher LS. Identification by combined gas chromatography-mass spectrometry of constituent long-chain fatty acids and alcohols from the meibomian glands of the rat and a comparison with human meibomian lipids. *J Chromatogr*. 1987;414:253–263.

22. Harvey DJ. Long-chain fatty acids and alcohols from gerbil meibomian lipids. *J Chromatogr*. 1989;494:23–30.

23. McFadden WH, Bradford DC, Eglinton G, Hajlbrahim SK, Nicolaides N. Application of combined liquid chromatography/mass spectrometry (LC/MS): analysis of petroporphyrins and meibomian gland waxes. *J Chromatogr Sci*. 1979;17:518–522.

24. Barnett KC, Sansom J. Dry eye in the dog and its treatment. *Trans Ophthalmol Soc U K*. 1985;104:462–466.

25. Butovich IA, Arciniega JC, Lu H, Molai M. Evaluation and quantitation of intact wax esters of human meibum by gas-liquid chromatography-ion trap mass spectrometry. *Invest Ophthalmol Vis Sci*. 2012;53:3766–3781.

26. Lin Z, Liu X, Zhou T, et al. A mouse dry eye model induced by topical administration of benzalkonium chloride. *Mol Vis*. 2011;17:257–264.

27. Lemp MA, Hamil JR. Factors affecting the tear film breakup in normal eyes. *Arch Ophthalmol*. 1973;89:103–105.

28. Stafford JH, Thorpe PE. Increased exposure of phosphatidylethanolamine on the surface of tumor vascular endothelium. *Neoplasia*. 2011;13:299–308.

29. McMahon A, Butovich IA, Kedzierski W. Epidermal expression of an Elovl4 transgene rescues neonatal lethality of homozygous Stargardt disease-3 mice. *J Lipid Res*. 2011;52:1128–1138.

30. Butovich IA. Cholesteryl esters as a depot for very long chain fatty acids in human meibum. *J Lipid Res*. 2009;50:501–513.

31. Butovich IA. Fatty acid composition of cholesteryl esters of human meibomian gland secretions. *Steroids*. 2010;75:726–733.

32. Nakamura S, Okada S, Umeda Y, Saito F. Development of a rabbit model of tear film instability and evaluation of viscosity of artificial tear preparations. *Cornea*. 2004;23:390–397.

33. Norn MS. Lissamine green. Vital staining of cornea and conjunctiva. *Acta Ophthalmol (Copenh)*. 1973;51:483–491.

34. Nicolaides N, Santos EC. The di- and triesters of the lipids of steer and human meibomian glands. *Lipids*. 1985;20:454–467.

35. Sonntag NOV. The reactions of aliphatic acid chlorides. *Chem Rev*. 1953;52:237–416.

36. Small DM. The effects of glyceride structure on absorption and metabolism. *Annu Rev Nutr*. 1991;11:413–434.

37. Gasser K, Fuchs-Baumgartinger A, Tichy A, Nell B. Investigations on the conjunctival goblet cells and on the characteristics of glands associated with the eye in the guinea pig. *Vet Ophthalmol*. 2011;14:26–40.

38. Kaswan R, Pappas C Jr, Wall K, Hirsh SG. Survey of canine tear deficiency in veterinary practice. *Adv Exp Med Biol*. 1998;438:931–939.

39. Westermeyer HD, Ward DA, Abrams K. Breed predisposition to congenital alacrima in dogs. *Vet Ophthalmol*. 2009;12:1–5.

40. Sanchez RF, Innocent G, Mould J, Billson FM. Canine keratoconjunctivitis sicca: disease trends in a review of 229 cases. *J Small Anim Pract*. 2007;48:211–217.

41. Butovich IA, Wojtowicz JC, Molai M. Human tear film and meibum. Very long chain wax esters and (O-acyl)-omega-hydroxy fatty acids of meibum. *J Lipid Res*. 2009;50:2471–2485.

42. Mishima S, Maurice DM. The effect of normal evaporation on the eye. *Exp Eye Res*. 1961;1:46–52.

43. Nakamura S, Okada S, Umeda Y, Saito F. Development of a rabbit model of tear film instability and evaluation of viscosity of artificial tear preparations. *Cornea*. 2004;23:390–397.

44. Moore CP, Wilsman NJ, Nordheim EV, Majors LJ, Collier LL. Density and distribution of canine conjunctival goblet cells. *Invest Ophthalmol Vis Sci*. 1987;28:1925–1932.

45. Blount WP. Studies of the movements of the eyelids of animals: blinking. *Quart J Exp Physiol*. 1927;18:112–125.

46. Jester JV, Nicolaides N, Smith RE. Meibomian gland studies: histologic and ultrastructural investigations. *Invest Ophthalmol Vis Sci*. 1981;20:537–547.

47. Jester BE, Nien CJ, Winkler M, Brown DJ, Jester JV. Volumetric reconstruction of the mouse meibomian gland using high-resolution nonlinear optical imaging. *Anat Rec (Hoboken)*. 2011;294:185–192.

48. Butovich IA, Uchiyama E, Di Pascuale MA, McCulley JP. Liquid chromatography-mass spectrometric analysis of lipids present in human meibomian gland secretions. *Lipids*. 2007;42:765–776.

49. Dean AW, Glasgow BJ. Mass spectrometric identification of phospholipids in human tears and tear lipocalin. *Invest Ophthalmol Vis Sci*. 2012;53:1773–1782.

50. Georgiev GA, Kutsarova E, Jordanova A, Krastev R, Lalchev Z. Interactions of meibomian gland secretion with polar lipids in Langmuir monolayers. *Colloids Surf B Biointerfaces*. 2010;78:317–327.